

# Green Chemistry

Cutting-edge research for a greener sustainable future

[rsc.li/greenchem](http://rsc.li/greenchem)

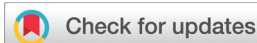


ISSN 1463-9262

## COMMUNICATION

Travis Williams, Steven Nutt *et al.*

A rapid electrochemical method to recycle carbon fiber composites using methyl radicals



Cite this: *Green Chem.*, 2023, **25**, 7058

Received 24th May 2023,  
Accepted 19th July 2023

DOI: 10.1039/d3gc01765f  
[rsc.li/greenchem](http://rsc.li/greenchem)

## A rapid electrochemical method to recycle carbon fiber composites using methyl radicals†

Zehan Yu, <sup>‡a</sup> Y. Justin Lim, <sup>‡b</sup> Travis Williams <sup>\*b</sup> and Steven Nutt <sup>\*a</sup>

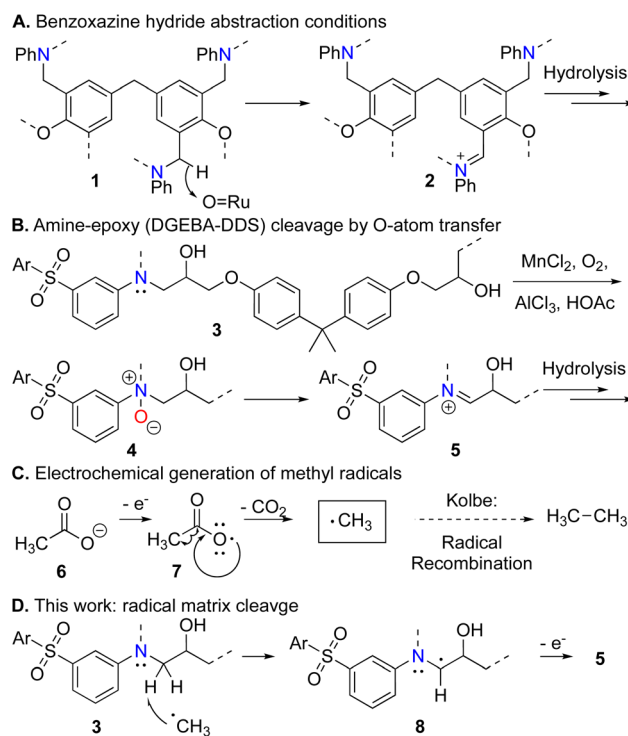
We introduce an electrochemical approach to recycle carbon fiber (CF) fabrics from amine-epoxy carbon fiber-reinforced polymers (CFRPs). Our novel method utilizes a Kolbe-like mechanism to generate methyl radicals from  $\text{CH}_3\text{COOH}$  to cleave C–N bonds within epoxy matrices *via* hydrogen atom abstraction. Recovered CFs are then remanufactured into CFRPs without resizing.

Thermoset carbon fiber reinforced polymer (CFRP) composites comprise a polymer matrix and carbon fibers (CFs) so that the combination imparts exceptional strength-to-weight, stiffness, and corrosion resistance relative to metallic alloys. Because of these properties, CFRPs are top choices for lightweight structural components in the aerospace, automobile, and wind energy industries. There has been a continuous increase in global demand for CFRPs, projected to reach 285 000 tons in 2025.<sup>1</sup> Thermoset CFRPs are cured irreversibly to produce a solid, crosslinked polymer matrix. Once the process completes, the matrix is insoluble and inert. Thus, recycling end-of-life (EOL) CFRPs is challenging.

We have previously introduced oxidative recycling processes for benzoxazine and amine-epoxy CFRPs based on ruthenium hydride abstraction<sup>2</sup> and peroxide<sup>3</sup> or  $\text{O}_2/\text{Mn}^{\text{II}}$  conditions,<sup>4</sup> respectively, each enabling both fiber and resin recovery and featuring analysis of chemical mechanism (Scheme 1A and B).<sup>5</sup> Building on these insights, we now present the first electrochemical method to deploy electrolysis-generated methyl radicals to depolymerize amine-epoxy CFRPs (Scheme 1). In this process, we use fibers imbedded within the CFRP as the anode to electrolyze  $\text{CH}_3\text{COOH}$  and generate

methyl radicals directly on the CFRP. Such radicals abstract hydrogen atoms adjacent to the polymer's linking nitrogen atom, thus, ultimately enabling selective C–N bond cleavage and completely dissolving CFRP matrices ( $T_g > 160$  °C) within 20 hours while preserving the fabric architecture of CFs. Fiber fabrics were then directly remanufactured to produce second-cycle CFRPs.

Electrochemical approaches to CFRP recycling have emerged that attempt to leverage the conductive CFs present in the composites. Currently, most electrochemical recycling methods use a CFRP as the anode to electrolyze chloride solutions. These methods reportedly generate chlorine-based oxides



Scheme 1 Approaches to cleave various CFRP matrices.

<sup>a</sup>MC Gill Composites Center, Mork Family Department of Chemical Engineering and Material Science, University of Southern California, 3651 Watt Way, Los Angeles, California, 90089, USA. E-mail: nutt@usc.edu

<sup>b</sup>Loker Hydrocarbon Research Institute, Wrigley Institute of Environmental Studies, and Department of Chemistry, University of Southern California, 837 Bloom Walk, Los Angeles, California, 90089, USA. E-mail: travisw@usc.edu

† Electronic supplementary information (ESI) available. See DOI: <https://doi.org/10.1039/d3gc01765f>

‡ Co-first author.

dants ( $\text{Cl}_2$ ,  $\text{HOCl}$ ,  $-\text{OCl}$ ) that degrade thermoset polymers and can also chlorinate imbedded fibers.<sup>6–8</sup> Alternative chlorine-free electrochemical methods involve phosphoric acid or a mixture of dimethyl sulfoxide (DMSO) and ammonium acetate.<sup>9,10</sup> These methods have lower efficiency, taking up to 21 days to complete, and tend to damage the fibers.

To our view, no satisfying mechanistic data have been reported on any electrochemical CFRP digest method. Previous studies have shown that photolysis-generated chlorine and hydroxyl radicals digest organic waste.<sup>11</sup> Some CFRP recycling studies have proposed to use radical-based reaction mechanisms to achieve efficient matrix digestion.<sup>12–15</sup> However, these studies did not characterize the reactive intermediate(s) or pathway of depolymerization. Here we will use a spin trap strategy to obtain structural information on our propagating radical(s).

Our method is based on a Kolbe-like electrolysis that generates methyl radicals to cleave C–H groups in an amine-epoxy matrix. Thus, acetic acid decomposes to methyl radicals as shown in Scheme 1C.<sup>16</sup> This happens on the carbon fiber electrode imbedded within the CFRP material. The transient radical mediates a curiously selective hydrogen atom abstraction, ultimately converting the matrix's linking amine to a hydrolysable imine (Scheme 1D).

We demonstrate this concept with two CFRPs, A and B, prepared with different amine-epoxy matrices (see ESI† for details). CFRP-A ( $T_g = 160^\circ\text{C}$ ) was produced in-house using diglycidyl ether of bisphenol A (DGEBA) epoxy and 3,3'-diaminodiphenyl sulfone (3,3'-DDS), as in Scheme 1B. CFRP-B samples ( $T_g = 197^\circ\text{C}$ ) were produced using a commercial prepreg of a similar structure (Solvay CYCOM 5320-1) to demonstrate the feasibility of recovering materials from an aerospace material.

Once fully cured, CFRPs laminates were cut to  $50.8 \times 10.2$  mm or  $76.2 \times 38.1$  mm for use as the anode, while a graphite rod served as the cathode (Scheme 2). The electrodes were immersed in an electrolyte solution containing  $\text{CH}_3\text{COOH}$ ,  $\text{NaCl}$ , and deionized water. Added  $\text{NaCl}$  assists electron transportation and enhance the conductivity of electrolyte solutions. Electrolysis reactions were performed at constant current (0.25 A) at  $110^\circ\text{C}$  for 20 hours under reflux with

various electrolyte concentrations, respectively summarized in Table 1. Entries 1–7 test the effect of  $\text{NaCl}$  and  $\text{CH}_3\text{COOH}$ . Entries 8 and 9 demonstrate feasibility of the method on our commercial CFRPs.

Clean CF fabrics are recovered after electrolysis. Fig. 1 shows light microscope images of fabrics recovered after 20 hours using conditions in Table 1. Images of entries 1–5 show more complete matrix removal with increasing  $\text{CH}_3\text{COOH}$  concentration (1.93–11.6 M) at constant  $\text{NaCl}$  concentration (1 M). Images of entries 5–8 reveal that increasing  $\text{NaCl}$  concentration (0.5–1 M) resulted in more complete matrix decomposition at constant  $\text{CH}_3\text{COOH}$  concentration (11.6 M). These show that higher  $[\text{CH}_3\text{COOH}]$  and  $[\text{NaCl}]$  reduced digestion times. Therefore, we chose 11.6 M  $\text{CH}_3\text{COOH}$  and 1 M  $\text{NaCl}$  (entries 5, 7 and 8).

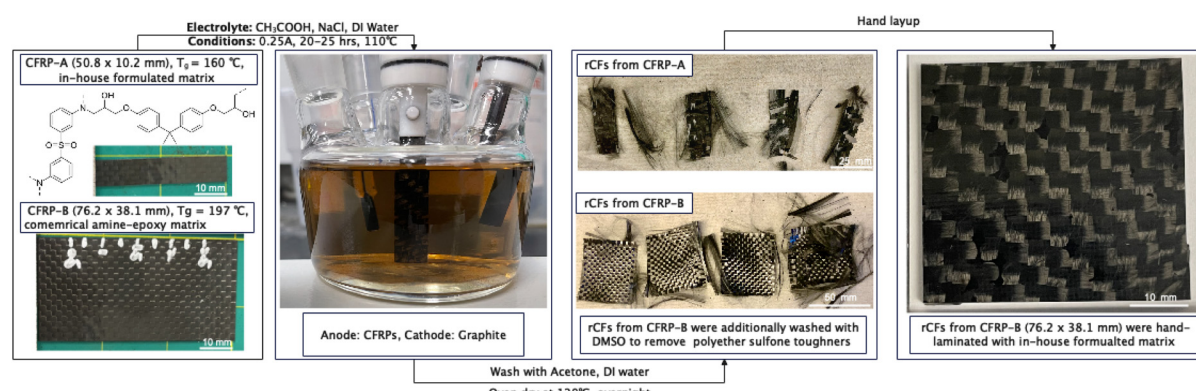
Fig. S2† shows the measured voltage of Table 1, entry 5 fluctuated between 4–6.5 V during the electrolysis. Thus, 4 V was selected as optimal, and we switched conditions to fixed voltage.

Single fiber tensile strength of fresh and recovered CFs was measured and data are summarized in Table S2 (see ESI for details).† The results show reclaimed CFs retained 94.24% of tensile strength and 83.43% of modulus.

Fig. 2 shows SEM images of virgin CF and recovered CFs from entries 5 and 8. Fig. 2(a) shows surface grooves characteristic of the virgin fibers. Fig. 2b and c demonstrate that the CFs were clean and undamaged by the electrolysis process. EDS composition analysis of virgin and CFs recovered from

**Table 1** Electrolysis CFRP digestion experiment summary

Entry	CFRP	$\text{CH}_3\text{COOH}(\text{M})$	$\text{NaCl}(\text{M})$
1	CFRP-A (50.8 × 10.2 mm)	1.93	1
2	CFRP-A (50.8 × 10.2 mm)	4.35	1
3	CFRP-A (50.8 × 10.2 mm)	6.77	1
4	CFRP-A (50.8 × 10.2 mm)	8.70	1
5	CFRP-A (50.8 × 10.2 mm)	11.6	1
6	CFRP-A (50.8 × 10.2 mm)	11.6	0.75
7	CFRP-A (50.8 × 10.2 mm)	11.6	0.5
8	CFRP-B (50.8 × 10.2 mm)	11.6	1
9	CFRP-B (76.2 × 38.1 mm)	11.6	1



**Scheme 2** Electrolysis recycling process for recovering and reusing CFs from amine-epoxy CFRPs.



Fig. 1 Light microscope images of recycled CFs from entries 1–8, showing matrix residue (white arrows).

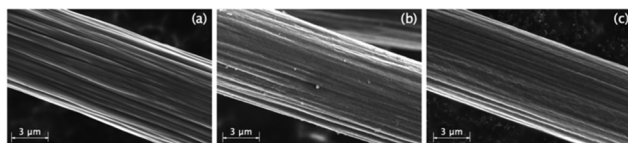


Fig. 2 SEM images of virgin CF (a) and recycled CFs from entries 5 (b) and 8 (c).

entry 5 is summarized in Table 2 and Fig. S5, 6:† after 20 hours of electrolysis, EDS data show no chlorine, and oxygen increased by <0.8 wt%, indicating no evidence of oxidation or chlorination on recovered CFs. An alternative electrolysis recycling method that involved chlorine reported surface chlorine content increased by up to 8 wt%.<sup>6</sup> The difference in surface chemistry implies that the active radical in our system is carbon-centered, not chlorine or oxygen, as implied elsewhere.

Scheme 2 also illustrates the process of recovering CF sheets from CFRP-B and remanufacturing them into second cycle CFRPs. First, CFRP-B ( $76.2 \times 38.1$  mm) samples were electrolyzed for 25 hours under optimized conditions. Recovered CF fabrics were washed successively with acetone, deionized water, and DMSO to remove excess reactants and polyether sulfone tougheners. After drying, cleaned fabrics were hand-laminated with in-house resin (as in CFRP-A). Remanufactured CFRPs were fully consolidated, demonstrating the viability of up-cycling in-tact CF fabric from electrolysis conditions.

We next attempted to spin trap our active radical. This approach utilizes a nitroxide spin trap to react with any radicals present to produce a long-lived adduct that can be analyzed by EPR and MS.<sup>17</sup> 5,5-Dimethyl-1-pyrroline-N-oxide (DMPO) was

used to capture and identify radicals. Radicals were generated in the presence and absence of matrix, the latter involving an experiment with a bare CF sheet. Finally, a representative surrogate of the matrix ( $\text{Bu}_4\text{DDS}$ ) was used to confirm that C–N bonds were the cleavage sites.

We first confirmed radical generation. Table 3 shows two trials with the spin trap DMPO using bare fiber (entry A1) and CFRP-A (entry A2) as the anode. EPR confirmed the presence of new radical adducts (Fig. S7†). Next, we compared the rates of conversion between entries A1 and A2. A sample of each entry was collected after 1 h electrolysis and analyzed by NMR. Despite paramagnetism of the nitroxide radical, structural details of DMPO ring were detectable. Fig. S9† shows comparison of the nitroxide signals in (a) pure DMPO, (b) entry A1, and (c) entry A2. The nitroxide signal at  $\delta = 7.5$  ppm remains in entry A2 but not A1, indicating that the presence of matrix greatly reduces the rate of conversion of DMPO. Thus, the radical is constrained around the matrix. This finding is supported by COSY NMR data, which also show no nitroxide signal for entry A1 (Fig. S10†).

To identify the propagating radical itself, a sample of entry A1 was analyzed by MS and showed three strong signals at  $m/z = 130$ , 172, and 194, as illustrated in Fig. 3. Positive control experiments were established for the methyl, hydroxyl, and chlorine DMPO radical adducts.

Using conditions shown in Table 4. Entries C1–3 respectively produced methyl, hydroxyl, and chlorine radicals that were respectively trapped cleanly by DMPO. Fig. 3 further shows the stacked mass data for each trapped radical species, including CFs experiment A1. The signal  $m/z = 130$  from A1 aligns only with the methyl radical adduct C1. The finding of methyl radicals is further supported by GC headspace analysis of experiment A1. This analysis reveals both methane and carbon dioxide (Fig. S15†), which is consistent with the formation of a methyl radical through a Kolbe-like process (Scheme 1C).

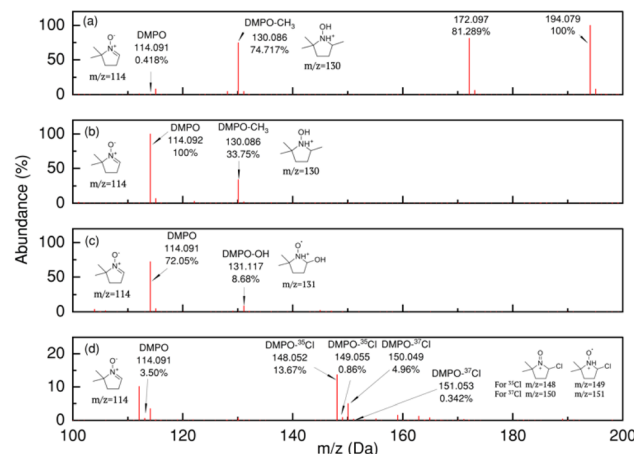
We further identified the site of matrix cleavage by using  $\text{Bu}_4\text{DDS}$ , a small molecule model of the matrix (Fig. S16†). Thus,  $\text{Bu}_4\text{DDS}$  was exposed to our electrolysis system for two hours, using a bare carbon fiber fabric anode. NMR tracked molecular changes; these conditions are laid out in Table 5 and Fig. S17.† We note a decrease in a signal at  $\delta = 3.29$ , which is characteristic of the  $\text{R}_2\text{N}-\text{CH}_2\text{R}$  group. The corresponding appearance of a  $\delta = 2.98$  signal represents mono-dealkylated  $\text{Bu}_3\text{DDS}$  and  $\text{N},\text{N}'\text{-Bu}_2\text{DDS}$ . We surmise that these products form via C–H atom abstraction, followed by oxidation to an iminium cation that hydrolyzes readily. Interestingly, while dealkylation proceeds all the way to primary anilines, no further degradation is observed. This assertion was proven

Table 2 EDS surface composition analysis of fiber surfaces

Sample	C (wt%)	N (wt%)	O (wt%)
Virgin CF	92.3	6.8	0.9
Recycled CF	93.8	4.5	1.7

Table 3 Active radical trapping experiment

Entry	Electrolysis conditions	Spin trap	Anode	Sampling time
A1	$\text{CH}_3\text{COOH}$ (11.6 M), $\text{NaCl}$ (1 M), 4 V, 60 °C	DMPO	CFs	1 h
A2			CFRP-A	



**Fig. 3** LC-QTOF spectrum of entries A1 (a), C1 (b), C2 (c), and C3 (d). Only entries A1 and C1 exhibit a strong signal for  $m/z = 130$ , confirming the production of methyl radicals.

**Table 4** LC-QTOF assignment and positive control experiment

Entry	Conditions	Spin trap	Adduct ( $m/z$ )
C1	$\text{C}_8\text{H}_{18}\text{O}_2$ (DTBP)	DMPO	130
C2	$\text{CuCl}_2$ , Hepes, $\text{H}_2\text{O}_2$	DMPO	131
C3	$\text{C}_8\text{H}_{12}\text{N}_4$ (AIBN), $\text{SO}_2\text{Cl}_2$	DMPO	148, 149, 150, 151

**Table 5**  $\text{Bu}_4\text{NDS}$  small molecule matrix model digestion experiments

Entry	Electrolysis conditions	Matrix	Anode	Sampling time
B1	$\text{CH}_3\text{COOH}$ (11.6 M), $\text{NaCl}$ (1 M)	$\text{Bu}_4\text{NDS}$	Graphite	1 h
B2	4 V, 60 °C			2 h

when we attempted to digest DDS and isolated unreacted DDS and acetylated DDS derivatives, the latter acetylated by the solvent (Fig. S18 and S19†).

Our combined data lead to a proposed mechanism for this process, shown in Scheme 1D. Methyl radicals are the active oxidant in the system, cleaving the  $\text{R}_2\text{N}-\text{CH}_2\text{R}$  bond by an initial hydrogen atom abstraction. This leads to iminium hydrolysis and selective bond cleavage at the polymeric C–N linkage.

In summary, we report an efficient electrochemical CRFP recycling method. Careful mechanistic studies hold that the process exploits methyl radicals, derived from solvent electro-oxidation, selectively to depolymerize amine-epoxy matrices to form recoverable fine chemicals. Unlike prior electrochemical methods, this radical-based technology achieves complete dissolution of high-performance CFRPs within 20 hours and yields clean CFs that are readily remanufactured into second-generation CFRPs. We confirm the presence of methyl radicals with the first application of spin trapping methodology in CRFP recycling. The study provides a new chemical recycling pathway using radicals to up-cycle high-performance composites.

## Conflict of interest

Williams is the founder of Closed Composites, a start-up aiming to commercialize composite materials recycling.

## Acknowledgements

This work is sponsored by the MC Gill Composites Center at USC and the National Science Foundation (CMMI-2134658). and TJW thanks NSF for BRITE award sponsorship (CMMI-2227649). We thank the NSF (CHE-2018740, DBI-0821671, CHE-0840366), the NIH (S10 RR25432), and USC Research and Innovation Instrumentation Awards for analytical tools. Huntsman Corporation and Solvay generously donated the epoxy, amine curing agent, and prepreg used in this study. We thank Brian Feng for taking SEM and EDS characterization and Jaideep Singh for EPR characterization.

## References

1. J. Zhang, G. Lin, U. Vaidya and H. Wang, *Composites, Part B*, 2022, 110463.
2. J. N. Lo, S. R. Nutt and T. J. Williams, *ACS Sustainable Chem. Eng.*, 2018, **6**, 7227–7231.
3. Y. Ma, D. Kim and S. R. Nutt, *Polym. Degrad. Stab.*, 2017, **146**, 240–249.
4. C. A. Navarro, Y. Ma, K. H. Michael, H. M. Breunig, S. R. Nutt and T. J. Williams, *Green Chem.*, 2021, **23**, 6356–6360.
5. C. A. Navarro, E. A. Kedzie, Y. Ma, K. H. Michael, S. R. Nutt and T. J. Williams, *Top. Catal.*, 2018, **61**, 704–709.
6. H. Sun, G. Guo, S. A. Memon, W. Xu, Q. Zhang, J.-H. Zhu and F. Xing, *Composites, Part A*, 2015, **78**, 10–17.
7. J.-H. Zhu, P.-Y. Chen, M.-N. Su, C. Pei and F. Xing, *Green Chem.*, 2019, **21**, 1635–1647.
8. K. Oshima, S. Matsuda, M. Hosaka and S. Satokawa, *Sep. Purif. Technol.*, 2020, **231**, 115885.
9. K. Oshima, M. Hosaka, S. Matsuda and S. Satokawa, *Sep. Purif. Technol.*, 2020, **251**, 117296.
10. C. Pei, P.-Y. Chen, S.-C. Kong, J. Wu, J.-H. Zhu and F. Xing, *Sep. Purif. Technol.*, 2021, **278**, 119591.
11. S. Xiao, J. Qu, X. Zhao, H. Liu and D. Wan, *Water Res.*, 2009, **43**, 1432–1440.
12. M. Das, R. Chacko and S. Varughese, *ACS Sustainable Chem. Eng.*, 2018, **6**, 1564–1571.
13. A. Yu, Y. Hong, E. Song, H. Kim, I. Choi and M. Goh, *J. Ind. Eng. Chem.*, 2022, **112**, 193–200.
14. D. H. Kim, M. Lee and M. Goh, *ACS Sustainable Chem. Eng.*, 2020, **8**, 2433–2440.
15. M. Lee, D. H. Kim, J.-J. Park, N.-H. You and M. Goh, *Waste Manage.*, 2020, **118**, 190–196.
16. F. J. Holzhäuser, J. B. Mensah and R. Palkovits, *Green Chem.*, 2020, **22**, 286–301.
17. M. J. Davies, *Methods*, 2016, **109**, 21–30.